THE AMERICAN SOCIETY OF MECHANICAL ENGINEERS
345 E. 47th St., New York, N.Y. 10017

95-GT-395

THROUGHFLOW METHOD FOR TURBOMACHINES APPLICABLE FOR ALL FLOW REGIMES

S. V. Damle and T. Q. Dang
Department of Mechanical and Aerospace Engineering
Syracuse University

D. R. Reddy
Internal Fluid Mechanics Division
NASA Lewis Research Center

ABSTRACT

A new axisymmetric throughflow method for analyzing and designing turbomachines is proposed. This method utilizes body-force terms to represent blade forces and viscous losses. The resulting equations of motion, which include these body-force terms, are casted in terms of conservative variables and are solved using a finite-volume time-stepping scheme. In the inverse mode, the swirl schedule in the bladed regions (i.e. the radius times the tangential velocity rV_θ) is the primary specified flow quantity, and the corresponding blade shape is sought after. In the analysis mode, the blade geometry is specified and the flow solution is computed. The advantages of this throughflow method compared to the current family of streamline curvature and matrix methods are that the same code can be used for subsonic/transonic/supersonic throughflow velocities, and the proposed method has a shock capturing capability. This method is demonstrated for designing a supersonic throughflow fan stage and a transonic throughflow turbine stage.

Nomenclature

b	blockage function (Eq. 7)
B	magnitude of the blade body-force (Eq. 4)
e_t	stagnation internal energy $(\mathbf{V}^2/2 + C_vT)$
f	blade wrap angle in radians
$\mathbf{F}_B$	blade body force (Eq. 1)
$\mathbf{F}_L$	viscous body force (Eq. 2)
H_o	stagnation enthalpy normalized to RT_{01}
I	rothalpy normalized to RT_{01}
L	loss distribution function (Eq. 3)
p	static pressure normalized to P_{01}
P_0	stagnation pressure normalized to P_{01}
R	ideal gas constant
(r, θ, z)	cylindrical coordinate system
s	entropy normalized to R
T	temperature normalized to T_{01}
T_0	stagnation temperature normalized to T_{01}
$\mathbf{V}$	absolute velocity normalized to $\sqrt{RT_{01}}$
$\mathbf{W}$	relative velocity normalized to $\sqrt{RT_{01}}$
α	blade surface in radians ($\alpha = \theta$ - f(r,z))
ρ	density normalized to P_{01}/RT_{01}
η_{st}	adiabatic stage efficiency
ω	rotational speed normalized to $\sqrt{RT_{01}}/r_{tip}$

Subscripts

(r, θ, z)	r, θ *and* z components
tip	at tip radius of rotor blade
1,2	conditions at inlet and outlet
s,p	suction and pressure surfaces

INTRODUCTION

Throughflow calculation methods are the most useful tools in the design of turbomachines (Cumpsty, 1989).

Presented at the International Gas Turbine and Aeroengine Congress & Exposition
Houston, Texas - June 5-8, 1995
This paper has been accepted for publication in the Transactions of the ASME
Discussion of it will be accepted at ASME Headquarters until September 30, 1995

These methods are most commonly used in the design mode. In this mode, the annulus and blade geometries are designed having prescribed the stagnation temperature rise/drop across the blade rows and some estimates of the blade row performance. Another application of these throughflow methods is the prediction of the flowfield given the annulus and blade profiles when used in the analysis mode.

There are two popular approaches for the throughflow calculation: the streamline curvature throughflow method (Smith, 1966) and the matrix throughflow method (Marsh, 1966). The streamline curvature throughflow method solves the so-called radial equilibrium equation which is casted in terms of primitive variables. The matrix throughflow method solves the so-called principal equation which is casted in terms of the streamfunction. Neither of these methods can deal with transonic or supersonic throughflow velocity accurately.

In view of recent developments and capabilities of simulating fully three-dimensional flows in multistage turbomachines with robust time-marching algorithms for the Euler/Navier-Stokes equations, the usefulness of integrating with them in a design system a time-marching throughflow method has been stressed. The idea of developing a throughflow method using the body-force field concept to represent blade rows in conjunction with existing time-marching algorithms for the Euler/Navier-Stokes equations was suggested by Miller & Reddy (1991). They proposed an axisymmetric viscous/inviscid "passaged-averaged" throughflow package to be integrated with their 3D design/analysis system for turbomachine blades - called the NASA LERC Turbomachinery Design/Analysis System.

In this paper, a formal theoretical development of a throughflow method based on the conservative-variable formulation is given. This method can be used to design and analyze multistage turbomachines in the axisymmetric limit and is applicable in the subsonic/transonic/supersonic flow regimes. In this paper, expressions are developed for the body-force terms used to model 1) the presence of blade rows, and 2) viscous effects via loss models. Other body-force terms such as those associated with the "passage-averaged" equations can in principle be included in this formulation (Adamczyk, 1985). Finally, the equations derived include a blockage term which can be used to model blade thickness and viscous effects.

The proposed throughflow method can be used in both the analysis and inverse modes. In the analysis mode, the blade profiles (actually the flow angle or the S2 streamsurface) are prescribed, and the axisymmetric flowfield is computed. In the design mode, the swirl schedule $rV_\theta(r,z)$ is prescribed in the bladed regions, and the blade profiles (actually the flow angle or the S2 streamsurface) are computed. The formulation of the proposed throughflow method is conceptually similar to the one proposed by Spurr (1980).

This paper is arranged as follows. The description of the theory is first presented. Next, the numerical techniques employed to solve the governing equations and the method of implementing boundary conditions are summarized. Results of two design studies, a supersonic throughflow fan stage and a transonic throughflow turbine stage, are then presented. Finally, concluding remarks are given.

THEORETICAL BACKGROUND

The use of a distributed body-force field to model turbomachine flowfield was first proposed by Marble (1964). This concept has been used extensively in throughflow methods (Dang & Wang, 1992; Denton, 1978; Hirsch & Warzee, 1976; Marsh, 1966). In a throughflow approximation, the body force can be seen to be composed of two components, one due to the pressure force exerted on the blades, and the other due to viscous and multistage effects. In this section, we develop expressions for the blade and viscous body forces.

Blade and viscous body force fields

The expression for the blade body-force field is first developed. We begin by noting two important characteristics of the blade body-force field. First, the blade body force must he zero everywhere except in the hladed region. Second, the blade body force must point in the direction normal to the blade surface since it represents entirely the reaction on the fluid of ideal pressure forces on the blades. On using these two properties, the blade-body force field denoted by $\mathbf{F}_B$ can be expressed as

$$\mathbf{F}_B = B(r,z)\nabla\alpha \qquad (1)$$

where the constant α surface defined as $\alpha = \theta - f(r,z)$ denotes the blade surface, and thus $\nabla\alpha$ is a vector normal to the blade surface (Dang & Wang, 1992). Conceptually, the constant α surface corresponds to the S2-surface concept proposed by Wu (1952), and it is approximately the hlade surface. In Eq. (1), the function B(r,z) is related to the change in the fluid's angular momentum imparted by the blade rows and/or viscous effects.

Next, an expression for the viscous body force is developed. In general, viscous losses occuring in the blade passage can be included in the body-force term

$\mathbf{F}_L$ which can be expressed as

$$\mathbf{F}_L = -L(r,z)\frac{\mathbf{W}}{|\mathbf{W}|} \tag{2}$$

This form models viscous effects as a retarding force which is opposite in direction to the local velocity direction, assuming that L(r,z) is positive. The function L(r,z) represents the magnitude of the viscous loss and can be varied depending on the degree of sophistication required.

The simplest loss model involves the specification of an entropy field distribution s(r,z) in the flow passage (Bosman & Marsh, 1974). In this case, the function L(r,z) can be related to the entropy field through Crocco's equation (see appendix)

$$L(r,z) = \frac{T}{|\mathbf{W}|}\mathbf{W}\cdot\nabla s \tag{3}$$

where T is the local static temperature. As an example, the entropy field can be constructed as follows. Given the adiabatic stage efficiency, the net mass-averaged entropy rise across the stage can be computed. In addition, if the shapes (i.e. not magnitude) of the radial variation in entropy increase at the outlet of the stage and the axial variation in entropy increase within the blade rows are given, then the entropy field can be constructed.

On using the expression for the viscous body force in Eq. (3), the magnitude of the blade body force B(r,z) can be derived. In the appendix, it is shown that the tangential component of the momentum equation yields an expression for the function B in Eq. (1)

$$B = \mathbf{V}\cdot\nabla(rV_\theta) + rL\frac{W_\theta}{|\mathbf{W}|} \tag{4}$$

In the case of a loss-free turbomachine (L=0), Eq. (4) states that the blade body force is related to the change in the fluid's angular momentum per unit mass along the meridional streamline. In the presence of viscous effects, Eq. (4) indicates that the strength of the blade body force is modified for a given increase in rV_θ. Finally, we note that the blade body force must vanish at the blade trailing edge (i.e. the Kutta condition) and outside the bladed region.

Equations of motion

The equations to be solved here are the axisymmetric unsteady equations of motion expressed in terms of the conservative variables, e.g.

$$\frac{\partial \mathbf{U}}{\partial t} + \frac{1}{r}\frac{\partial(r\mathbf{E})}{\partial r} + \frac{\partial \mathbf{G}}{\partial z} = \rho b(\mathbf{S} + \mathbf{S}_B + \mathbf{S}_L) \tag{5}$$

In Eq. (5), the conservative-variable vector **U**, the flux vectors **E** and **G**, and the source vector **S** are defined as

$$\mathbf{U} \equiv \begin{bmatrix} b\rho \\ b\rho V_r \\ b\rho V_\theta \\ b\rho V_z \\ b\rho e_t \end{bmatrix} \quad \mathbf{E} \equiv \begin{bmatrix} b\rho V_r \\ b(\rho V_r^2 + p) \\ b\rho V_r V_\theta \\ b\rho V_r V_z \\ b\rho V_r H_o \end{bmatrix}$$

$$\mathbf{G} \equiv \begin{bmatrix} b\rho V_z \\ b\rho V_z V_r \\ b\rho V_z V_\theta \\ b(\rho V_z^2 + p) \\ b\rho V_z H_o \end{bmatrix} \quad \mathbf{S} \equiv \begin{bmatrix} 0 \\ ((p+\rho V_\theta^2)/r + \frac{p}{b}\frac{\partial b}{\partial r})/\rho \\ -V_r V_\theta / r \\ (p/\rho b)\frac{\partial b}{\partial z} \\ 0 \end{bmatrix} \tag{6}$$

In the above relations, b=b(r,z) is the blockage factor which can be used to model blade thickness and takes on the form

$$b(r,z) = 1 - \frac{\theta_p - \theta_s}{2\pi/N_b} \tag{7}$$

where (θ_p - θ_s) represents the blade thickness in radian, and N_b is the numher of blades. The source vector $\mathbf{S}_B$ models the blade rows as a distributed body-force field. On using Eqs. (1) and (4), the source vector $\mathbf{S}_B$ takes on the form

$$\mathbf{S}_B = \begin{bmatrix} 0 \\ \mathbf{F}_B\cdot\hat{\mathbf{e}}_r \\ \mathbf{F}_B\cdot\hat{\mathbf{e}}_\theta \\ \mathbf{F}_B\cdot\hat{\mathbf{e}}_z \\ \mathbf{V}\cdot\nabla H_o \end{bmatrix} = \begin{bmatrix} 0 \\ -[\mathbf{V}\cdot\nabla(rV_\theta^*) + rL\frac{W_\theta}{|\mathbf{W}|}]\frac{\partial f}{\partial r} \\ [\mathbf{V}\cdot\nabla(rV_\theta^*) + rL\frac{W_\theta}{|\mathbf{W}|}]/r \\ -[\mathbf{V}\cdot\nabla(rV_\theta^*) + rL\frac{W_\theta}{|\mathbf{W}|}]\frac{\partial f}{\partial z} \\ \omega[\mathbf{V}\cdot\nabla(rV_\theta^*)] \end{bmatrix} \tag{8}$$

In Eqs. (6) and (8), both V_θ and V_θ^* denotes the tangential velocity component. However, these quantities are to be interpreted as follows. The quantity V_θ is computed using the θ-component of the momentum equation (i.e. third component of Eq. (5)). On the other hand, the quantity V_θ^* is prescribed in the inverse mode and is evaluated using the flow-tangency condition in the analysis mode. Clearly, in the inverse mode, when the solution converges, the computed value of rV_θ is identically equal to the prescribed rV_θ^* distribution.

The source vector $\mathbf{S}_L$ models viscous losses as a distributed body-force field. On using Eq. (2), the source vector $\mathbf{S}_L$ takes on the form

$$\mathbf{S}_L = \begin{bmatrix} 0 \\ \mathbf{F}_L\cdot\hat{\mathbf{e}}_r \\ \mathbf{F}_L\cdot\hat{\mathbf{e}}_\theta \\ \mathbf{F}_L\cdot\hat{\mathbf{e}}_z \\ 0 \end{bmatrix} = \begin{bmatrix} 0 \\ -L\frac{W_r}{|\mathbf{W}|} \\ -L\frac{W_\theta}{|\mathbf{W}|} \\ -L\frac{W_z}{|\mathbf{W}|} \\ 0 \end{bmatrix} \tag{9}$$

Finally, we note that in Eq. (5), we have neglected all the perturbations terms that would result from circumferentially averaging the equations of motion (Jennions & Stow, 1985). However, these correlation terms can easily be incorporated into the equations as source terms. Other effects such as correlations associated with the average-passage equation system of Adamczyk (1985) can also be included in the equations as source terms.

The inverse mode

In the inverse mode, the swirl distribution $rV_\theta^*(r,z)$ is prescribed in the bladed regions. The computed quantities are the blade profiles as described by f(r,z). This quantity is obtained by enforcing the flow-tangency condition along the blade surface, viz

$$\mathbf{W}\cdot\nabla\alpha = 0 \longrightarrow V_r\frac{\partial f}{\partial r}+V_z\frac{\partial f}{\partial z} = \frac{V_\theta^*}{r} - \omega \quad (10)$$

In the inverse mode, f is updated periodically during the time-marching process of the unsteady equations of motion (i.e. Eq. (5)) to steady state. The new value for f is then used to update the source vector $\mathbf{S}_B$ given in Eq. (8). In order to solve the above initial-value problem, a boundary condition for f needs to be prescribed. This boundary condition is taken from the prescribed blade stacking position (Dang & Wang, 1992).

We note that tbe swirl distribution rV_θ^* is a useful quantity to prescribe in the inverse mode because it is directly related to the work input/output of the rotor blades (i.e. from the Euler Turbine Equation). For the stator vanes, the swirl distribution is the most appropriate quantity to prescribe because the function of these vanes is to remove swirl (in a compressor) or add swirl (in a turbine) to the flow.

The analysis mode

In the analysis mode, the blade geometry function f(r,z) is prescribed and the flow solution is computed. In this mode, the magnitude of tbe blade body force is adjusted so that the flow-tangency condition is satisfied. This is accomplished by adjusting the blade body force through $rV_\theta^*(r,z)$ in Eq. (8) using the flow-tangency condition along tbe blade surface. This condition yields the following algebriac relation

$$\mathbf{W}\cdot\nabla\alpha = 0 \longrightarrow rV_\theta^* = r^2(\omega + V_r\frac{\partial f}{\partial r}+V_z\frac{\partial f}{\partial z}) \quad (11)$$

In the analysis mode, the quantity rV_θ^* is computed periodically during the time-marcbing process of the unsteady equations of motion (i.e. Eq. (5)) to steady state. The new value for rV_θ^* updated using Eq. (11) is used to update the source vector $\mathbf{S}_B$ given in Eq. (8).

NUMERICAL TECHNIQUE

The unsteady equations of motion given in Eq. (5) is marched to steady-state using the cell-centered finite-volume Runge-Kutta time-stepping scheme proposed by Jameson et al. (1981). This scheme consists of discretizing the integral form of Eq. (5) using a finite-volume technique which reduces to a centered-difference approximation on a uniform square grid. Blended nonlinear second- and fourth-difference artificial dissipation are needed to prevent oscillations in the numerical solutions. The resulting system of ODE's is then integrated using the explicit four-stage Runge-Kutta time-stepping scheme. The details of this algorithm is not given here and can be found in Jameson et al. (1981). We note that no acceleration technique was implemented in our computer code.

Boundary Conditions at Inflow Boundary

The usual method of imposing boundary conditions based on the theory of incoming and outgoing characteristic waves is adopted here. If the incoming flow is supersonic, then all five characteristics variables are specified at the inflow boundary. In the present study, we specify the following conditions at the inflow boundary: the stagnation pressure P_{01}, the stagnation temperature T_{01}, the Mach number M_1, the radial velocity V_{r1} and the tangential velocity $V_{\theta 1}$. If the incoming flow is subsonic, then four flow conditions can be specified at tbe inflow boundary, and one flow condition is extrapolated from tbe solutions inside the computational domain. In the present study, we specify $P_{01}, T_{01}, V_{r1}, V_{\theta 1}$, and we extrapolate the static pressure p_1 using a first-order space-extrapolation technique.

Boundary Conditions at Outflow Boundary

The same procedure based on tbe theory of incoming and outgoing characteristic waves is used at the outflow boundary. If the exit flow is supersonic, then all five characteristics variables must be extrapolated from tbe solutions inside the computational domain. In the present study, we extrapolate the five conservative variables using a first-order space-extrapolation technique. If the exit flow is subsonic, tben one characteristic variable must be specified, and the remaining four charateristic variables must be extrapolated from the solutions inside the computational domain. In the present study, we specify tbe exit static pressure p_2, and we extrapolate for the remaining four primitive variables.

Boundary Conditions along Hub and Shroud

The slip condition is imposed along the hub and shroud boundaries. In the cell-centered formulation, the mass, momentum and energy fluxes across the cell

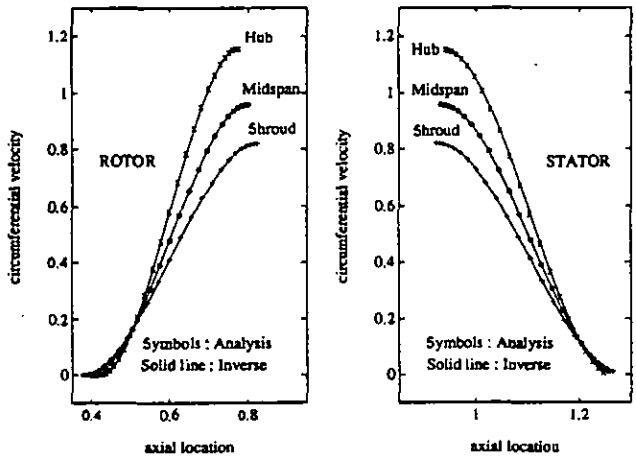

Figure 1: Comparison of V_θ axial distribution for STF fan stage (normalized to $\sqrt{RT_{01}}$).

boundaries coinciding with the hub and shroud are set to zero, and the pressure force acting on these boundaries are extrapolated from the cell-centered values.

RESULTS

The first example presented is the design and analysis of a single-stage Supersonic ThroughFlow (STF) fan. This fan has performance specifications similar to the one designed at NASA Lewis (Schmidt et al., 1987). In this design, the annulus has constant hub and shroud radii, with the hub-to-tip radius ratio of 0.7. In order to keep the blade solidity relatively constant at all radial locations, the blade axial chord is increased in the radial direction. The fan stage has 44 rotor blades and 52 stator blades. The rotor rotational speed ω (normalized to $\sqrt{RT_{01}}/r_{tip}$) is set at 1.575, the overall change in rV_θ across the rotor (normalized to $r_{tip}\sqrt{RT_{01}}$) is set at 0.815, and the adiabatic stage efficiency η_{st} is assumed to be 90% (a relatively high number for a STF fan stage). These inputs yield a designed fan pressure ratio of 2.7. The mesh employed in the following calculations has 96 cells in the axial direction and 24 cells in the radial direction.

The solid lines in Fig. 1 show the prescribed axial distributions of the tangential velocity V_θ in the rotor and stator regions along the hub, midspan, and shroud stations. Both rotor and stator blades are designed using free-vortex distributions. The rotor is designed to increase the fluid angular momentum per unit mass rV_θ from 0 to 0.815, and the stator is designed to deswirl the flow completely (Fig. 2).

In the bladed regions, the prescribed blockage function b(r,z) varies between 85% at the hub and 95% at the tip. This blockage function is used to model the blockage effect due to blade thickness. No flow blockage was imposed in non-bladed regions. Figure 3 illustrates the prescribed entropy field employed in this calculation. This loss distribution was generated by assuming an adiabatic stage efficiency of 90%. The loss is equally divided in the stator and rotor regions, and is proportioned more at the hub/shroud regions than at the midspan region.

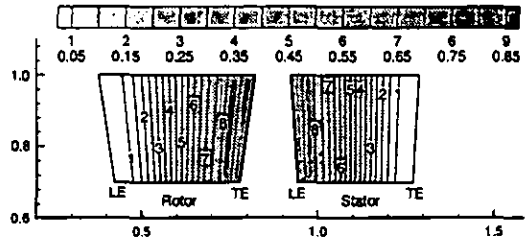

Figure 2: Prescribed rV_θ for STF fan stage (normalized to $r_{tip}\sqrt{RT_{01}}$).

Figure 4 illustrates the blade geometries calculated by the inverse mode. Figure 5 shows the contour plot of the absolute Mach number. This figure shows the presence of a high Mach-number region in the stator at the hub (maximum Mach number is on the order of 3.3), indicating the potential existence of high shock losses for this design.

For completeness, numerical results of the Mach number, static pressure and blade angle at the leading and trailing edges are tabulated in Table 1 at the hub/midspan/shroud locations.

STF fan		Rotor		Stator	
		LE	TE	LE	TE
Relative/ Absolute Mach No.	hub	2.32	2.69	3.21	3.29
	midspan	2.48	2.67	2.88	2.97
	shroud	2.66	2.72	2.72	2.58
Static Pressure p/P_{01}	hub	0.136	0.070	0.054	0.044
	midspan	0.133	0.094	0.093	0.078
	shroud	0.131	0.109	0.115	0.131
Blade Angle (degree)	hub	-32	1	27	0
	midspan	-37	-9	23	0
	shroud	-42	-18	20	0

Table 1: STF fan stage design results.

Next, the analysis mode of the code is used to verify the solutions given by the inverse mode. To carry out this consistency check, the flowfield through the STF

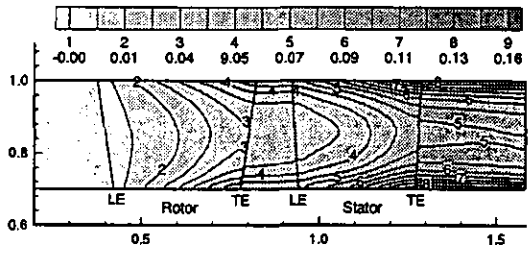

Figure 3: Prescribed entropy field for STF fan stage (normalized to gas constant R).

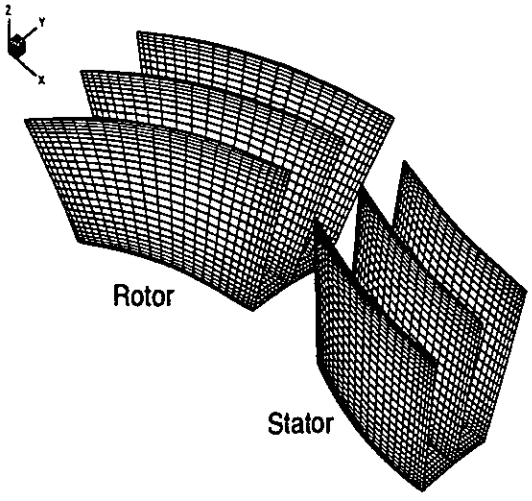

Figure 4: Designed STF blade geometries.

fan blade shown in Fig. 4 is analyzed using the analysis mode of the code. This consistency check is carried out to confirm that the designed blade profiles do produce the prescribed swirl distributions. Figure 1 illustrates excellent comparisons of the axial distributions of the tangential velocity V_θ at the hub/midspan/shroud locations between the prescribed values in the inverse mode (solid lines) and the values predicted by the analysis mode (symbols). Other results such as the Mach number and the static pressure also show excellent agreements between the results given by the inverse and analysis calculations.

Finally, we present an attempt to improve this STF fan design. This task is carried out to demonstrate the shock-capturing capability of the proposed throughflow method. The present design can be improved in two areas. First, the Mach number contour shown in Fig. 5 suggests the need to reduce the Mach number in the stator along the hub in order to minimize shock losses

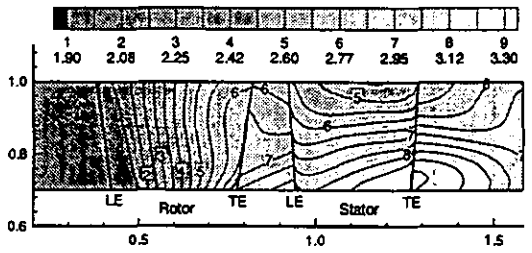

Figure 5: Absolute Mach number for STF fan stage.

which are inherent in the blade-to-blade plane. Second, the numerical results show that the average exit static pressure is well below the inlet static pressure. The inlet static pressure (normalized to P_{01}) is 0.13, and the average outlet static pressure is on the order of 0.08. In an actual engine design, the flow is slowed down in the diffuser through a weak oblique shock wave before entering the fan. Then, the bypass flow leaving the fan is expanded through a nozzle to ambient pressure. Hence, the exit static pressure should only be slightly lower than the fan inlet static pressure. To correct for these deficiencies, we propose to modify the hub geometry. Since the flow is supersonic in the stator region, we can improve this design by simply reducing the flow area in the stator region. The reduction in flow area will result in the deceleration of the flow and the accompanied increase in static pressure. We note that since the flow is supersonic, the contouring of the hub geometry must be done carefully to minimize shock losses.

Figure 6 and Figure 7 illustrate comparisons of the absolute Mach number and static pressure about three different designs. DESIGN A is the original design with constant hub and shroud radii. DESIGN B and DESIGN C both have constant tip radius. However, the hub radius (normalized to r_{tip}) in DESIGN C is chosen to vary smoothly from 0.7 at the inlet to 0.78 at the outlet, while the hub radius in DESIGN B varies from 0.7 at the inlet to 0.8 at the outlet at a faster rate than DESIGN C. These design calculations were carried out with the same swirl and blockage distributions as in the previous STF fan design study. However, the viscous loss model was removed from these calculations to isolate the effects of entropy rise across shocks which may be present in the new design (i.e DESIGN B and DESIGN C).

The contour plots shown in Figs. 6 and 7 indicate that the hub geometry in DESIGN C is an improved design over the original design (DESIGN A) in terms of (1) reducing the maximum Mach number in the stator region (maximum Mach number is reduced from 3.3 to 3.0), and (2) increasing the exit static pressure (the av-

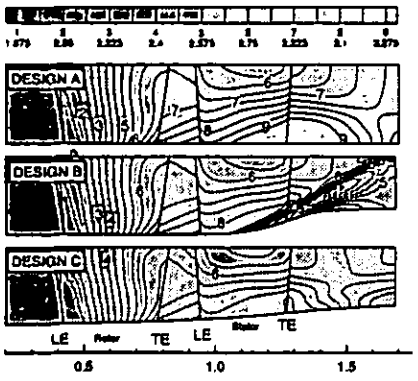

Figure 6: Comparison of absolute Mach number for STF fan stage.

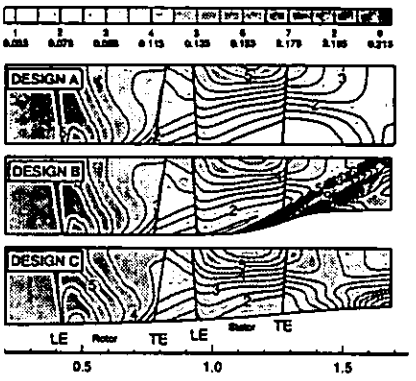

Figure 7: Comparison of static pressure for STF fan stage (normalized to P_{01}).

erage exit static pressure is increased from 0.08 to 0.12). In DESIGN B, although the region of high Mach number is also reduced, a strong oblique shock appears at the stator midchord location along the hub. Figure 8 illustrates a comparison of the entropy field for these three designs. This figure clearly shows the presence of a strong oblique shock in DESIGN B, while DESIGN C has no shock. We note that the magnitude of the entropy rise across this oblique shock is higher than the input viscous loss employed in the previous STF fan design (Fig. 3), indicating that shock losses in DESIGN B reduce the stage efficiency significantly. In fact, the calculated stage stagnation pressure ratio in DESIGN A and DESIGN C is 2.93, while the calculated stage stagnation pressure ratio in DESIGN B is 2.6.

The use of the proposed throughflow method to improve the STF fan-stage design illustrates the unique capability of the method to handle flows with strong shocks. Existing throughflow methods (streamline curvature and matrix methods) would not have been able to predict the oblique shock in DESIGN B. In the design stage of the turbomachine annulus in supersonic-flow applications, the shock-capturing capability is very important since the throughflow method must be able to differentiate between shocked and shock-free design. We note that even though shocks present in axisymmetric throughflow solutions may not be accurate since the actual flow is fully three-dimensional, preventing the appearance of shock waves in throughflow solutions will likely reduce shock losses in the "real" three-dimensional problem.

The second example to be presented is the design of a generic transonic throughflow turbine stage. In this study, the rotor rotational speed ω is set at 0.92, the overall change in rV_θ across the rotor is set at -

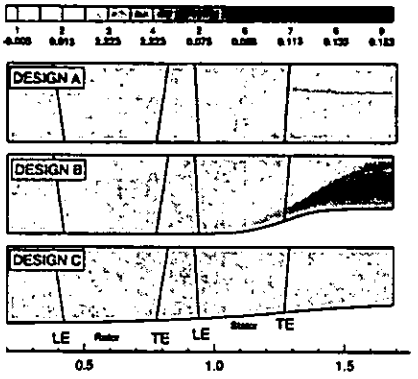

Figure 8: Comparison of entropy for STF fan stage (normalized to gas constant R).

0.73, and the stage efficiency η_{st} is assumed to be 87%. These inputs correspond to a designed stage stagnation pressure ratio of 0.40. The mesh distribution employed in this calculation has 90 cells in the axial direction and 20 cells in the radial direction.

The prescribed swirl distribution for this turbine stage is similar in shape to the one used in the STF fan, although the magnitude is different. In this example, the stator is designed to increase the fluid angular momentum per unit mass rV_θ from 0 to 0.73, and the rotor is designed to convert all the tangential momentum to shaft power. Both stator and rotor blades are designed using free-vortex distributions. The prescribed blockage function b(r,z) varies between 55% at the hub and 85% at the tip. The loss distribution was generated by assuming an adiabatic stage efficiency of 87%. The loss is equally divided in the stator and rotor regions,

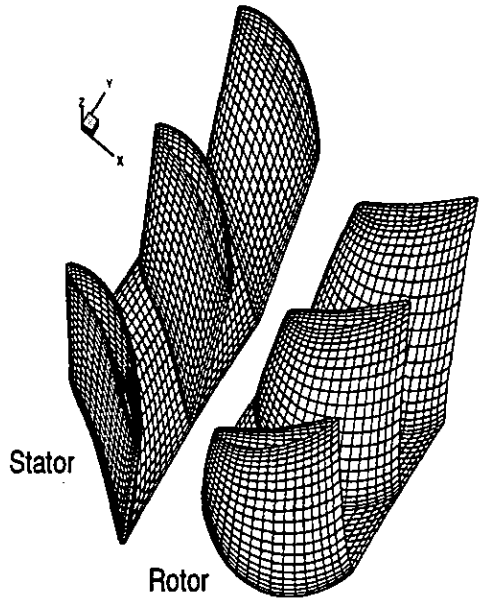

Figure 9: Designed turbine blade geometries.

and is proportioned more at the hub/shrould regions than at the midspan region.

Figure 9 illustrates the blade geometries calculated by the inverse mode. The designed turbine stage has 36 stator blades and 46 rotor blades. Figure 10 shows the contour plot of the absolute Mach number in the meridional plane. This figure shows the presence of a supersonic-flow region in the intra-bladed region along the hub. For completeness, numerical results of the Mach number, static pressure and blade angle at the blade leading and trailing edges are tabulated in Table 2 at the hub/midspan/shroud locations.

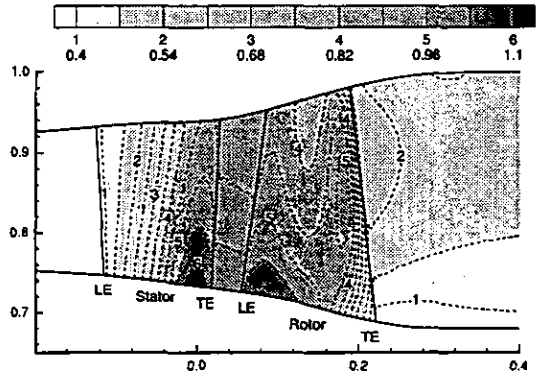

Figure 10: Absolute Mach number for transonic turbine stage.

Turbine		Stator		Rotor	
		LE	TE	LE	TE
Relative/ Absolute Mach No.	hub	0.31	1.05	1.01	0.74
	midspan	0.33	0.98	0.91	0.98
	shroud	0.36	0.92	0.88	1.11
Static Pressure p/P_{01}	hub	0.917	0.435	0.460	0.344
	midspan	0.912	0.494	0.531	0.299
	shroud	0.913	0.520	0.545	0.295
Blade Angle (degree)	hub	0	62	36.4	-56.8
	midspan	0	56.3	12.5	-49.3
	shroud	0	50.7	-10.6	-52.9

Table 2: Transonic turbine fan stage design results.

CONCLUDING REMARKS

A newly-developed throughflow method for turbomachine flowfield design/analysis using modern shock-capturing techniques is proposed. This method utilizes body-force terms to represent the presence of blade rows and viscous losses. Expression for the blade body force is derived from the basic flow equations. To demonstrate the capability of the method to handle viscous effects, a simple viscous loss model is used to represent losses via a body-force term. The method solves the time-dependent equations of motion, casted in terms of the conservative variables and included the body-force terms, using a four-stage Runge-Kutta time-stepping scheme and a finite-volume formulation. The primary advantages of this throughflow method over the conventional streamline curvature and matrix throughflow methods are that 1) transonic and supersonic throughflow velocities can readily be computed, and 2) a shock-capturing technique is available.

The proposed throughflow method can be used in both the inverse and analysis modes. In the analysis mode, the annulus and blade geometries are prescribed, and the method calculates the axisymmetric flowfield. In the inverse mode, the annulus along with the swirl schedules in the bladed regions are prescribed, and the method calculates the corresponding blade geometries and the remaining flow solutions. In this paper, design studies of a Supersonic ThroughFlow (STF) fan stage and a transonic throughflow turbine stage are presented. The STF fan-stage design studies include design calculations with strong shocks.

As the purpose of this work is to introduce a newly-developed throughflow method for the design/analysis of turbomachine flowfields, several assumptions are used in this initial study. For example, the blade deviation angles are taken to be zero so that the flow angles are assumed to be the same as the blade angles. Also, the loss model employed in this study is relatively rudi-

mentary. With the use of these assumptions, it is clear that the method in its present form does not provide a reliable design tool, and no comparison with test data are presented in this paper.

ACKNOWLEDGEMENTS

This research was supported by the NASA Lewis Research Center under grant NAG3-1585 (Dr. David Miller - Technical Monitor) and the CASE Center at Syracuse University. The authors would like to thank David Allen and Richard Ziomkowski for their assistance in carrying out the STF-fan calculations.

Appendix

Viscous body force

The general form of the Crocco's equation is

$$-\mathbf{W} \times (\nabla \times \mathbf{V}) = -\nabla I + T\nabla s + \mathbf{F}_B + \mathbf{F}_L$$

Substituting the expressions for the blade and viscous body forces given in Eqs. (1) and (2) into the above equation, we have

$$-\mathbf{W} \times (\nabla \times \mathbf{V}) = -\nabla I + T\nabla s + B\nabla\alpha - L\frac{\mathbf{W}}{|\mathbf{W}|}$$

On taking the dot product of $\mathbf{W}$ with the above equation, and noting that $\mathbf{W} \cdot \nabla I$ is zero from the conservation law of rothalpy along streamlines (Lyman, 1993), and that $\mathbf{W} \cdot \nabla\alpha$ is zero from the flow tangency condition along the hlade surfaces, we obtain

$$L(r,z) = \frac{T}{|\mathbf{W}|}\mathbf{W} \cdot \nabla s$$

We note that since the entropy always increases along the direction of flow, L is always positive as required by the loss model.

Blade body force

The momentum equation for steady flow is

$$\rho(\mathbf{V} \cdot \nabla)\mathbf{V} = -\nabla p + \rho\mathbf{F}_B + \rho\mathbf{F}_L$$

On using the expressions for the body force terms given in Eqs. (1) and (2), the θ-component of the above equation reads, for axisymmetric flows

$$V_\theta V_r + rV_r\frac{\partial V_\theta}{\partial r} + rV_z\frac{\partial V_z}{\partial z} = B - rL\frac{W_\theta}{|\mathbf{W}|}$$

Solving for B yields

$$B(r,z) = \mathbf{V} \cdot \nabla rV_\theta + rL\frac{W_\theta}{|\mathbf{W}|}$$

Outside the bladed region, B vanishes and the above equation reduces to

$$\mathbf{V} \cdot \nabla rV_\theta = -rL\frac{V_\theta}{|\mathbf{V}|}$$

In the absence of viscous losses, the above equation is a statement of conservation of angular momentum along a streamline. When losses are present, the entropy increases along the direction of flow and the above equation shows that the angular momentum decreases in the direction of flow (Bosman & Marsh, 1974).

References

Adamczyk, J. J., 1985, "Model Equation for Simulating Flows in Multistage Turbomachinery," ASME Paper No. 85-GT-226.

Bosman C. and Marsh H., 1974, "An Improved Method for Calculating the Flow in Turbo-Macbines, Including a Consistent Loss Model," *Journal of Mechanical Engineering Science*, vol. 16, no. 1, pp. 25-31.

Cumpsty, N. A., 1989, *Compressor Aerodynamics*, Longman Scientific & Technical.

Dang, T. Q. and Wang, T., 1992, "Design of Multi-Stage Turbomachinery Blading by the Circulation Metbod: Actuator Duct Limit," ASME Paper No. 92-GT-286.

Denton J. D., 1978, "Throughflow Calculations for Transonic Axial Flow Turbines," ASME *Journal of Engineering for Power*, vol. 100, pp. 212-218.

Hirsch, C. and Warzee, G., 1976, "A Finite-Element Method for Through-Flow Calculations in Turbomachines," ASME *Journal of Fluids Engineering*, pp. 403-421.

Jameson, A., Schmidt, W. and Turkel, E, 1981, "Numerical Solution of the Euler Equations by Finite Volume Methods Using Runge-Kutta Time-Stepping Schemes," AIAA Paper No. 8I-1259.

Jennions, I. K. and Stow, P., 1985, "The Quasi-Three-Dimensional Turbomachinery Blade Design System, Part I :Throughflow Analysis, Part II : Computerized System," ASME *Journal of Engineering for Gas Turbines and Power*, vol. 107, pp. 301-314.

Lyman, F. A., 1993, "On Conservation of Rotbalpy in Turbomachines," ASME *Journal of Turbomachinery*, vol. 115, pp. 520-526.

Marble, F. E, 1964, "Tbree-Dimensional Flow in Turbomachine," *High Speed Aerodynamics and Jet Propulsion*, vol. 10, sec. C, Princeton University Press, pp. 83-166.

Marsh, H., 1966, "A Digital Computer Program for the Through-Flow Fluid Mechanics in an Arbitrary Turbomachine using a Matrix Method," Aeronautical Research Council, R&M 3509.

Miller, D. and Reddy, D. R., 1991, "The Design/Analysis of Flows through Turbomachinery - A Viscous/Inviscid Approach," AIAA Paper No. 91-2010.

Schmidt, J. F., Royce, M. D., Wood, J. R. and Steinke, R. J., 1987, "Supersonic Through-Flow Fan Design," AIAA Paper No. 87-1746.

Smith, L. H., 1966, "The Radial-Equilibrium Equation of Turbomachinery," ASME *Journal of Engineering for Power,* pp. 1-12.

Spurr, A., 1980, "The Prediction of 3D Transonic Flow in Turbomachinery Using a Combined Through-flow and Blade-to-Blade Time Marching Method," *International Journal of Heat and Fluid Flow*, vol. 2, no. 4, pp. 189-199.

Wu, C. H., 1952,"A General Theory of Three-Dimensional Flow in Subsonic and Supersonic Turbomachines of Axial, Radial and Mixed-Flow Types," NACA TN 2604.